



Anomalous effects in charging of Pd powders with high density hydrogen isotopes

Kitamura, Akira ; Nohmi, Takayoshi ; Sasaki, Yu ; Taniike, Akira ; Takahashi, Akito ; Seto, Reiko ; Fujita, Yushi

(Citation)

Physics Letters A, 373(35):3109-3112

(Issue Date)

2009-08-24

(Resource Type)

journal article

(Version)

Accepted Manuscript

(URL)

<https://hdl.handle.net/20.500.14094/90001369>



Anomalous Effects in Charging of Pd Powders with High Density Hydrogen Isotopes

Akira Kitamura^{1*}, Takayoshi Nohmi¹, Yu Sasaki¹, Akira Taniike¹,
Akito Takahashi², Reiko Seto², and Yushi Fujita²

¹ Division of Marine Engineering, Graduate School of Maritime Sciences, Kobe University
5-1-1 Fukaeminami-machi, Higashinada-ku, Kobe 6580022, Japan

² Technova Inc., 1-1-1 Uchisaiwai-cho, Chiyoda-ku, Tokyo 1000011, Japan

*E-mail address: kitamura@maritime.kobe-u.ac.jp

Abstract

A twin system for hydrogen absorption experiments has been constructed to replicate the phenomenon of heat and ^4He generation by D_2 gas absorption in nano-sized Pd powders reported by Arata and Zhang, and to investigate the underlying physics. For Pd-Zr oxide nano-powders, anomalously large energies of hydrogen isotope absorption, 2.4 ± 0.2 eV/D-atom and 1.8 ± 0.4 eV/H-atom, as well as large loading ratio of $\text{D/Pd} = 1.1 \pm 0.0$ and $\text{H/Pd} = 1.1 \pm 0.3$, respectively, were observed in the phase of deuteride/hydride formation. The sample charged with D_2 also showed significantly positive output energy in the second phase after the deuteride formation.

Keywords: Pd-Zr nano-powder, Deuterium absorption, Hydrogen absorption, D/Pd ratio, Isotope effect

1. Introduction

Arata and Zhang recently reported that highly pure D₂ gas charging of Pd nano-powders in the form of Pd/ZrO₂ nano-composite induced significantly higher temperatures inside the reactor vessel than on the outside wall for more than 50 hours, while runs with H₂ gas showed almost no temperature difference [1]. To verify that the excess heat originated in a nuclear process, a QMAS was employed to show the existence of ⁴He as nuclear ash in the vessel and in the powder after the charging. The charging system is a sophisticated and simplified version of the previous-generation DS reactor [2]. Replication experiments using systems similar to the DS reactor with Pd-black seem to be successful [3,4].

However, few reports on the replication experiments producing heat and ⁴He with the new configuration have published yet in spite of extreme importance of the phenomenon. It is crucial to confirm the phenomenon of heat and ⁴He generation with fully quantitative reliability.

In the present work we constructed an experimental system to replicate the phenomenon and to investigate the underlying physics. We report here the first results of deuterium/hydrogen absorption and accompanying heat generation, which show anomalously large isotope effect.

2. Experimental procedure

An oxide sample of mixture of Pd (34.6 %) and Zr (65.4 %) was fabricated by Santoku Corporation, Kobe, Japan, and has an average particle size of 7.7 μm, a specific surface area of 37.1 m²/g, and an average Pd grain size of 10.7 nm. If we assume perfect oxidation of the metal elements, 10 g of the sample contains 3.0 g of Pd.

The D₂/H₂ absorption system is composed of two identical chambers (an A₁-A₂ twin system): one for a D₂ gas foreground run, and the other for H₂ gas background run. As shown in Fig.1, each part has an inner reaction chamber containing Pd powder and an outer chamber that is evacuated to provide thermal insulation for calorimetry. A sheath heater and a cooling water pipe made of copper are wound on the outer surface of the reaction chamber for baking the sample powder and for flow calorimetry to estimate the heat production rate, respectively. A pair of thermocouples is provided for the flow calorimetry by measuring the temperature difference between the inlet and the outlet of the cooling water.

The D₂ gas is nominally 99.5 % pure and the H₂ is 99.998 % pure. Flow rate control of D₂/H₂ gas purified through a liquid-nitrogen cold trap is made with a Pd membrane filter which

also serves as an additional purifier. The Pd membrane (0.2 mm-t, 99.95 %) separates the evacuated reaction chamber (50 mℓ) and the gas reservoir filled with D₂/H₂ at 1 MPa. The gas permeation rate is controllable between 0.1 and 25 sccm by varying the membrane temperature from the room temperature to 900 K.

In expectation of occurrence of some nuclear phenomena, a neutron counter and a scintillation probe for γ -ray detection are located just outside the outer chambers. All parameters measured are stored in a PC with an acquisition period of 1 min.

As a calibration of the flow calorimeter, we measured the heat recovery rate under a variety of conditions; with input power of 1, 3, 6 and 10 W, and D₂ gas pressure of 0, 0.1, 0.3 and 1.0 MPa in the reaction chamber. The coolant flow rate was 6 mℓ/min in all cases. The heat recovery rate was found to be almost independent of the pressure and the input power, and the averaged value is $(63.1 \pm 5.8) \%$. Temperature response to a stepwise variation of the input power was found to be expressed as a simple exponential function with a time constant of 5.2 min.

We examined temperature uncertainty and drift, with no sample powder put in the A₁ chamber filled with H₂ gas at a pressure of 1 MPa. The inlet-outlet temperature difference and the output power deduced from it showed short-term fluctuation as shown in Fig. 2. If we regard an experimental error in the present system as the standard deviation of the longitudinal data, the error or the uncertainty for the output power and the integrated output energy measured for the A₁-A₂ system is evaluated to be 0.014 W and 0.83 kJ for 1000-min acquisition. In the prototype system A₀, which had the larger time constant and smaller sensitivity of heat measurement, and was used in the 1st stage experiments with the 0.1- $\mu\text{m}\phi$ Pd powder and the Pd-black [5], a temperature drift observed sometimes resulted in the larger error of 4.0 kJ for 1000-min run.

In the following, the run number is designated by “G-PN#M”, with G, P, N and M being the gas species, the powder species, powder ID, and the number of repeated use, respectively. The powder species include PP (Pd powder with particle diameter of 0.1 μm and a purity of 99.5 %), PB (Pd-black with a particle size of “300 mesh” and purity of 99.9 %), and PZ (mixed oxides of Pd-Zr). For example, “D-PB2#3” represents the third absorption run with D₂ using a Pd-black sample “2” following evacuation and baking after two cycles of evacuation-baking-absorption.

3. Results and discussion

3.1. 0.1- $\mu\text{m}\phi$ Pd powder

First of all, we describe absorption runs using the A_0 system for five gram of commercially available 0.1- $\mu\text{m}\phi$ Pd powder. The reaction chamber filled with the powder was evacuated and heated for baking at 430 K. Then highly pure D_2 or H_2 gas was introduced into the reaction chamber through the Pd membrane filter. The results for the case of D_2 and H_2 absorption are compared in Fig. 3(a). After the gas is introduced, pressure does not begin to rise for a while. During this phase (the first phase) the Pd powder absorbs almost all of the D_2 (H_2) gas atoms as they flow in, and heat is released as a result of adsorption and formation of deuterides (hydrides). After about 30 minutes, the powder almost stops absorbing gas; the gas pressure begins to rise, and the heat release from deuteride (hydride) formation subsides. This is the beginning of the 2nd phase, and the gas flow rate in the 1st phase is evaluated from the rate of the pressure increase. From the flow rate multiplied by the duration of the 1st phase, loading is estimated to reach $\text{PdD}_{0.43}$ ($\text{PdH}_{0.44}$).

The output powers are integrated over the 1st phase to give the output energies of 0.10 kJ/g-Pd(D) and 0.08 kJ/g-Pd(H), which are divided by the loading ratio of 0.43 and 0.44 to give the heat of solution ΔH_s of 0.24 eV/atom-D and 0.20 eV/atom-H, respectively. The values appear to be somewhat larger than those found in literatures [6 - 10]. However, they are consistent with each other, when we take into account that the differential heat of solution is a decreasing function of the loading ratio; $\Delta H_s = 0.15, 0.12, 0.070$, and 0.061 eV/H for H/Pd ratio of 0.5, 0.55, 0.6 and 0.65 [9,10]. The difference between D and H, the isotope effect, is rather large, but is not considered to be anomalous, since we find $\Delta H_s(\text{D})/\Delta H_s(\text{H}) = 1.25$ in ref. [9]. On the other hand, the output energies in the 2nd phase, *i.e.*, the output powers integrated over the 2nd phase with duration of 1,400 min, are smaller than the experimental error mentioned above, and is not meaningful. The results are summarized in Table I, which includes those for the Pd-black and the Pd-Zr mixed oxide samples.

3.2. 300-mesh Pd-black

The second kind of the sample tested is commercially available 300-mesh Pd-black whose surface has a kind of nano-scale fractal structure finer than the 0.1- $\mu\text{m}\phi$ Pd powder. The performance of the Pd-black absorption of D_2 using the A_0 system is compared with that of H_2 in Fig. 3(b). It is very interesting to note that: (1) much higher loading to $\text{PdD}_{0.88}$ or $\text{PdH}_{0.79}$ is realized, and (2) the output energies in the 1st phase, $E_{1\text{st}} = (0.67 \pm 0.12)$ eV/atom-D and (0.62 ± 0.11) eV/atom-H, are 2 - 3 times larger than those for the 0.1- $\mu\text{m}\phi$ Pd powder and

those found in the literatures [6 – 10]. On the other hand, the output energy of 8.3 ± 4.5 kJ (2.6 ± 1.4 kJ/g-Pd) in the 2nd phase of D₂ absorption appears to be larger than that in the case of H₂. The difference is only marginal compared with the above-mentioned error due to the temperature drift of 5.5 kJ in the present case.

Using the improved twin system A₁·A₂, we compared the performance of the Pd-black sample PB3 with a prolonged duration of the 2nd phase of 4,500 min, which was subjected to repeated use with the sample baking before absorption made at 440 K for 3 h (#2), or at 570 K for 1 h (#3). The results are shown in the 6th row through the 8th in Table I.

First we notice that the first run (D-PB3#1) has essentially the same D/Pd ratio and the energy output E_{1st} as those with the A₀ system. Second the repeated use retains almost the same or even higher energy output E_{1st} in spite of the significantly smaller D(H)/Pd ratio. This interesting fact could be related to some structural change of the sample. The SEM photograph of the sample indicated clumping together and disappearance of the fine structure on the scale of several tens of nm. This point will be discussed in detail later elsewhere. As for the 2nd phase, we have little to discuss, when we take into account that they are comparable to the error of 4.0 kJ/1000-min mentioned above for the A₀ system.

3.3. Mixed oxides of Pd·Zr

Now we describe the performance of the mixed oxides of Pd·Zr that are thought to have even finer mesoscopic structure. The results of six runs using virgin PZ samples are summarized in the last 6 rows in Table I. Those of runs with repeated use of the PZ sample will be found later together with the above-mentioned PB samples. Using the A₁·A₂ twin system, the runs H-PZ(2n)#1 were performed simultaneously with D-PZ(2n-1)#1, where $n = 1, 2$, and 3. The A₁ subsystem was used for D-PZ1#1, D-PZ3#1 and H-PZ6#1. In all runs, the PZ sample used was 10 g, and the baking temperature was 570 K for 3 h. The output energy in the 2nd phase is the power integrated over 1,600 min. Examples of the evolution of the output power and the pressure for runs D-PZ1#1 and H-PZ2#1 are shown in Fig. 3(c).

We notice the following four facts in the 1st phase: (1) very large output energies that are more than 3 times greater than those for the Pd-black samples, (2) very large D/Pd (H/PD) ratio of 1.1 ± 0.0 (1.1 ± 0.3) that are even higher than those for the PB samples, (3) surprisingly large $E_{1st} = (2.4 \pm 0.2)$ eV (D) and (1.8 ± 0.4) eV (H) on the average, and (4) larger isotope effect in E_{1st} compared with those for 0.1- $\mu\text{m}\phi$ powder and Pd-black; the difference just exceeds the error range determined from standard deviations.

We have anomalously large absorption energies and loading ratios accompanied by a large isotope effect in the present mesoscopic system of Pd-Zr oxides. It is difficult to assume large contribution of ZrO_2 to these quantities. We have to consider reduction of PdO_x followed by production of $x\text{D}_2\text{O}$ ($x\text{H}_2\text{O}$) and PdD_y (PdH_y). The reaction energies Q_D and Q_H are evaluated to be $(162.6 \times x + 70.0 \times y)$ kJ and $(156.6 \times x + 58.0 \times y)$ kJ, respectively. For assumed values of $x = 1 \sim 0$ and $y = 0 \sim 1$, Q_D and Q_H are $0.84 \sim 0.73$ eV/D and $0.81 \sim 0.60$ eV/H, respectively. These are too small to account for both the observed energy and the isotope effect.

There might be a yet-unknown atomic/electronic process governing the phenomenon in the present mesoscopic system, or the concept of “atom clusters” [11] might apply. However, it seems rather difficult to assume that such a large isotope effect is only in the electronic process of adsorption and/or hydride formation. Some nuclear process could be a candidate for the process responsible for the phenomenon.

As for the 2nd phase, we have negative values for the specific output energy in two runs using H_2 . This should be considered to be due to slight shift in the zero point of the thermocouple signal. In contrast to the runs with H_2 , the second phase in the runs with D_2 has apparently positive output energy as typically shown in Fig. 3(c). This implies that some nuclear process could be involved, although the values are only marginal in view of the negative value observed in H-PZ2#1. These points should be subjected to further investigation.

Finally, it should be mentioned that we observed nothing other than steady background both in the neutron counter and the scintillation probe.

4. Conclusion

Using the twin system, characteristics of deuterium/hydrogen absorption and accompanying heat generation have been compared for three kinds of Pd powders; the 0.1- $\mu\text{m}\phi$ Pd powder, the Pd-black, and the mixed oxides of Pd-Zr. It has been found that the D(H)/Pd ratio and absorption energy is an increasing function of fineness of the sample surface. For the Pd-black, loading to $\text{PdD}_{0.88}$ or $\text{PdH}_{0.79}$ and the output energies in the 1st phase, $E_{1\text{st}} = (0.67 \pm 0.12)$ eV/atom-D or (0.62 ± 0.11) eV/atom-H, were both 2 - 3 times larger than those for the 0.1- $\mu\text{m}\phi$ Pd powder and those found in the literatures.

Moreover, for Pd-Zr oxide nano-powders, anomalously large energies of hydrogen isotope absorption, $E_{1\text{st}} = (2.4 \pm 0.2)$ eV/D-atom or (1.8 ± 0.4) eV/H-atom, as well as large loading ratio of $\text{D/Pd} = 1.1 \pm 0.0$ or $\text{H/Pd} = 1.1 \pm 0.3$, respectively, were observed in the phase of

deuteride/hydride formation. The sample charged with D_2 also showed significantly positive output energy in the second phase after the deuteride formation.

References

- [1] Y. Arata and Y. Zhang: The special report on research project for creation of new energy, J. High Temperature Society, 2008, No. 1.
- [2] Y. Arata, and Y. Zhang: *Condensed Matter Nuclear Science, Proc. 12th Int. Conf. on Cold Fusion* (ed. A. Takahashi, Y. Iwamura, and K. Ota, World Scientific, 2006) pp.44-54.
- [3] V. A. Kirkinskii, A. I. Kumelnikov: *Proc. ICCF13, Sochi, 2007* (Publisher Center MATI, Moscow, ISBN 978-5-93271-428-7) pp.43-46.
- [4] J. P. Biberian and N. Armanet: *ibid.* pp.170-180.
- [5] T. Nohmi, Y. Sasaki, T. Yamaguchi, A. Taniike, A. Kitamura, A. Takahashi, R. Seto, and Y. Fujita: <http://www.ler-canr.org>; to be published in Proc. 14th Int. Conf. Condensed Matter Nuclear Science (ICCF14), Washington DC, 2008.
- [6] *Hydrogen in Metals II -Topics in Applied Physics*, **29**, ed. G. Alefeld and J. Voelkl (Springer, 1978).
- [7] A. Koiwai, A. Itoh, and T. Hioki: Japan Patent 2005-21860 (P2005-21860A).
- [8] C. P. Chang, *et al.*: *Int. J. Hydrogen Energy*, **16** (1991) 491.
- [9] M. M. Antonova: *Sboistva Gidriedov Metallov* (Properties of Metal-hydrides) (Naukova Dumka, Kiev, 1975; translated by NissoTsushinsha, Wakayama, 1976) [in Japanese].
- [10] Y. Fukai, K. Tanaka, and H. Uchida: *Hydrogen and Metals* (Uchida Rokakuho, Tokyo, 1998) [in Japanese].
- [11] H. Fujita: *J. High Temperature Society* **24** (1998) 272.

Figure captions

Fig. 1. (a) Reduced view of the $A_1 \cdot A_2$ twin system, and (b) functional view of A_1 .

Fig. 2. Blank run with no sample powder.

Fig. 3. Evolution of heat and pressure in the vessel after introduction of D_2 gas (blue/light blue) or to H_2 gas (red/pink); (a) $0.1\text{-}\mu\text{m}\phi$ Pd powder (D-PP1#1 and H-PP2#1), (b) 300-mesh Pd-black (D-PB1#1 and H-PB2#1), and (c) mixed oxides of Pd and Zr (D-PZ1#1 and H-PZ2#1).

Table I. Comparison of absorption runs for the 0.1- $\mu\text{m}\phi$ Pd powder (PP), the 300-mesh Pd-black (PB), and the Pd-Zr nano-composite (PZ).

Run #	weight of Pd [g]	Flow rate [sccm]	Output energy [kJ]		Specific output energy [kJ/g]		D/Pd or H/Pd (1st ph.)	E1st [eV/D(H)]
			1st phase	2nd phase	1st phase	2nd phase		
D-PP1#1	5.0	2.7	0.5 \pm 0.4	2.5 \pm 4.1	0.10 \pm 0.07	0.52 \pm 0.83	0.43	0.26 \pm 0.14
D-PP1#2	5.0	3.8	0.5 \pm 0.2	4.0 \pm 4.4	0.10 \pm 0.05	0.79 \pm 0.88	0.44	0.25 \pm 0.09
H-PP2#1	5.0	5.4	0.4 \pm 0.2	2.6 \pm 3.9	0.08 \pm 0.03	0.53 \pm 0.80	0.44	0.20 \pm 0.07
D-PB1#1	3.2	3.6	1.7 \pm 0.3	8.3 \pm 4.5	0.54 \pm 0.10	2.60 \pm 1.40	0.88	0.67 \pm 0.12
H-PB2#1	3.6	4.2	1.6 \pm 0.3	(-2.2 \pm 4.6)	0.45 \pm 0.08	(-0.62 \pm 1.30)	0.79	0.62 \pm 0.11
D-PB3#1	20.0	2.9	9.3 \pm 1.1	1.1 \pm 0.5	0.47 \pm 0.06	0.06 \pm 0.02	0.79	0.65 \pm 0.08
D-PB3#2	20.0	0.9	3.3 \pm 0.5	3.4 \pm 2.6	0.17 \pm 0.03	0.17 \pm 0.13	0.23	0.79 \pm 0.05
H-PB3#3	20.0	2.1	3.2 \pm 0.2	14 \pm 4.6	0.16 \pm 0.01	0.68 \pm 0.24	0.24	0.74 \pm 0.05
D-PZ1#1	3.0	1.8	7.0 \pm 0.2	6.8 \pm 1.3	2.33 \pm 0.05	2.27 \pm 0.43	1.08	2.4 \pm 0.05
H-PZ2#1	3.0	2.3	3.6 \pm 0.1	(-5.1 \pm 1.4)	1.20 \pm 0.02	(-1.70 \pm 0.47)	1.00	1.3 \pm 0.02
D-PZ3#1	3.0	1.9	6.4 \pm 0.2	6.2 \pm 1.4	2.13 \pm 0.05	2.07 \pm 0.47	1.08	2.2 \pm 0.05
H-PZ4#1	3.0	3.6	4.8 \pm 0.1	1.9 \pm 1.4	1.60 \pm 0.02	0.63 \pm 0.47	0.86	2.1 \pm 0.03
D-PZ5#1	3.0	2.0	7.1 \pm 0.2	1.3 \pm 1.4	2.38 \pm 0.03	0.42 \pm 0.45	1.04	2.5 \pm 0.03
H-PZ6#1	3.0	5.9	7.1 \pm 0.1	(-0.2 \pm 1.4)	2.36 \pm 0.02	(-0.08 \pm 0.48)	1.34	1.9 \pm 0.02
Average for PZ		(D) (H)	6.9 \pm 0.4 5.2 \pm 1.8	4.8 \pm 3.0 (-1.1 \pm 3.6)	2.3 \pm 0.1 1.7 \pm 0.6	1.6 \pm 1.0 (-0.4 \pm 1.2)	1.1 \pm 0.0 1.1 \pm 0.3	2.4 \pm 0.2 1.8 \pm 0.4

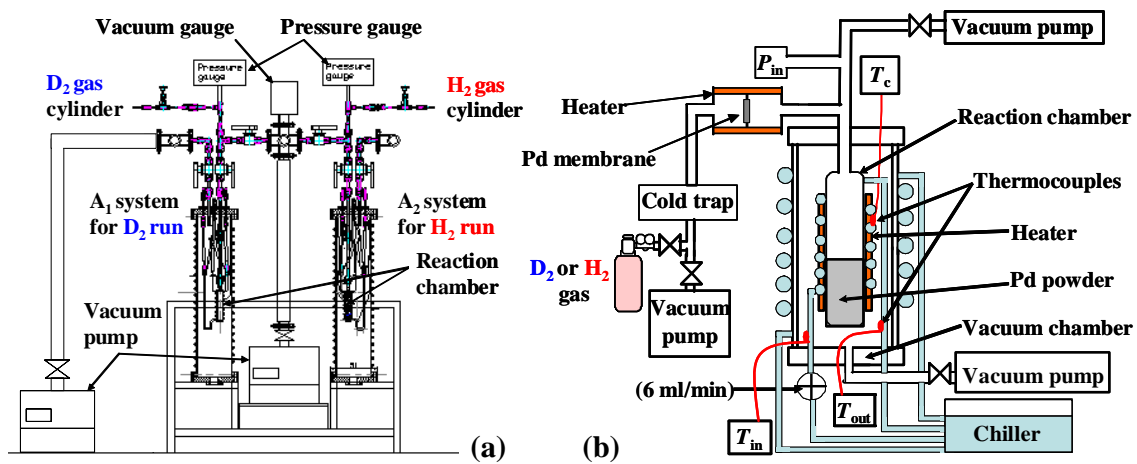


Fig. 1

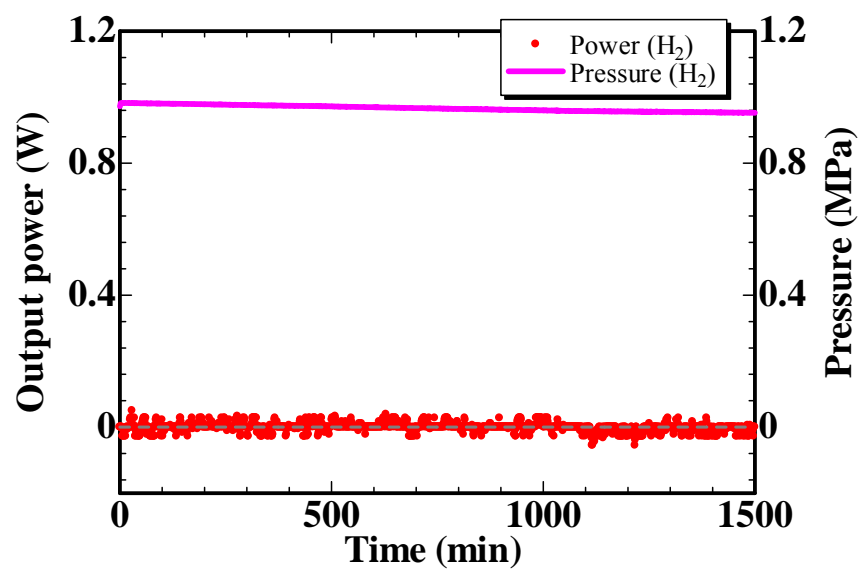


Fig. 2

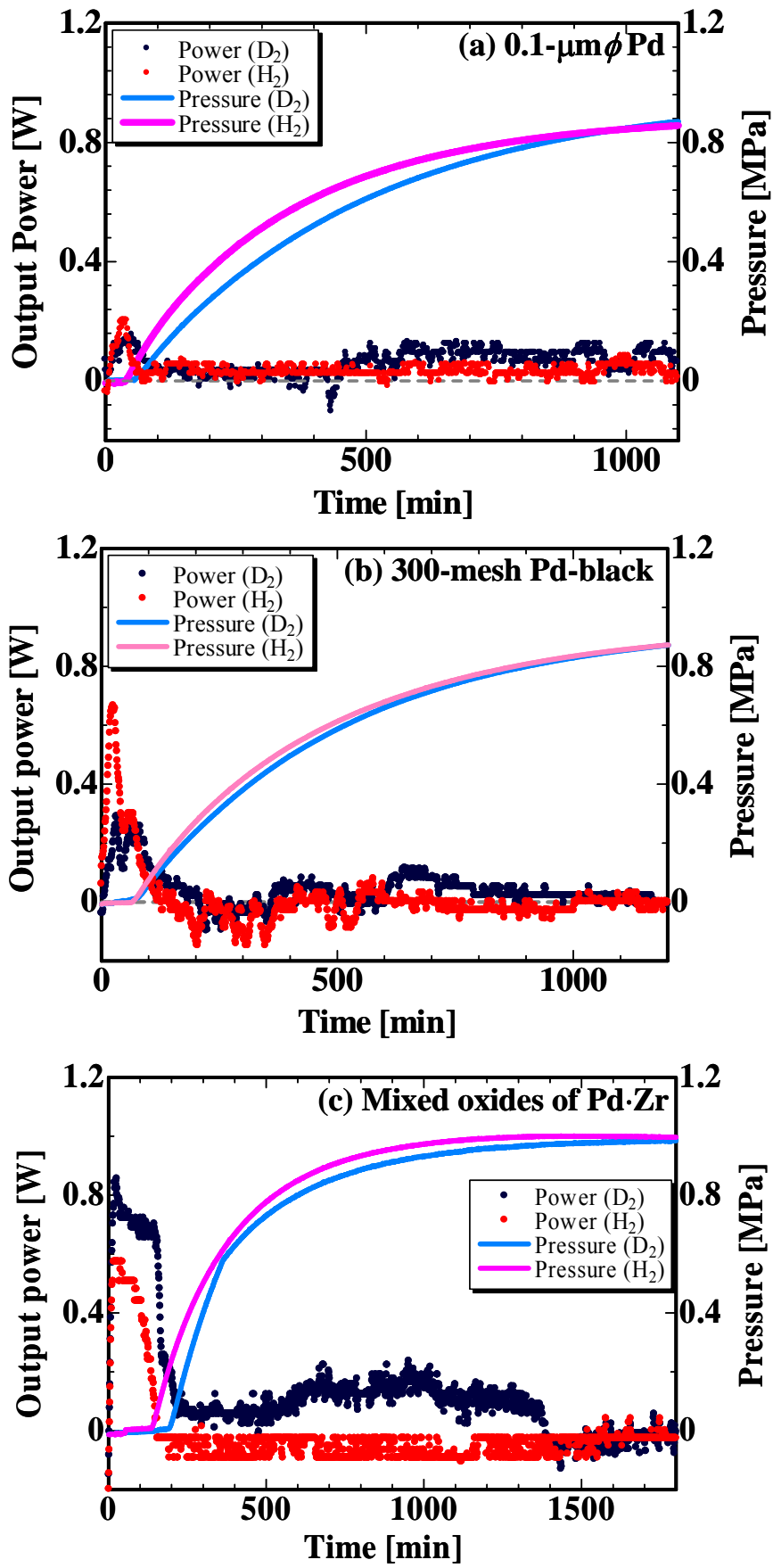


Fig. 3